Shaping Emission Spectra of Fluorescent Molecules with Single Plasmonic Nanoresonators

M. Ringler,[1] A. Schwemer,[1] M. Wunderlich,[1] A. Nichtl,[2] K. Kürzinger,[2] T. A. Klar,[1,3] and J. Feldmann[1,*]
[1]*Photonics and Optoelectronics Group, Physics Department and CeNS, Ludwig-Maximilians-Universität München, Amalienstraße 54, 80799 Munich, Germany*
[2]*Roche Diagnostics GmbH, Nonnenwald 2, 82372 Penzberg, Germany*
[3]*Institute of Physics and Institute of Micro- and Nanotechnologies, Technical University of Ilmenau, 98684 Ilmenau, Germany*

(Received 13 December 2007; published 22 May 2008)

We show that plasmonic nanoresonators composed of two gold nanoparticles change not only the intensity but also the spectral shape of the emission of fluorescent molecules. The plasmonic resonance frequency can be tuned by varying the distance between the nanoparticles, which allows us to selectively favor transitions of a fluorescent molecule to a specific vibrational ground state. Experimental data from correlated scattering and fluorescence microscopy agree well with calculations in the framework of generalized Mie theory. Our results show that the widely used description of a dye molecule near a metal surface as a mere two-level system is inadequate.

DOI: 10.1103/PhysRevLett.100.203002 PACS numbers: 37.30.+i, 52.25.Os, 73.20.Mf, 81.07.Pr

An electromagnetic resonator strongly modifies spontaneous emission of fluorescence in its spatial and spectral proximity [1]. The change in the local mode density of the electromagnetic field causes an enhancement or suppression of the overall emission rate [2]. In a multilevel system, such as a fluorescent molecule, resonant transitions are enhanced and nonresonant transitions are suppressed. Therefore, not only the overall emission rate but also the emission spectrum is changed [3].

Far-field standing-wave resonators can be miniaturized down to half the wavelength of light (so-called microcavities). With plasmonic near-field resonators this limit can be overcome. Single nanoparticles have been used successfully to modify spontaneous emission rates [4]. However, single nanoparticles only provide limited tunability through variation of the particle shape, size, or composition [5]. A nanoparticle dimer resonator allows finer and more flexible tuning by variation of the interparticle distance [6,7]. Thus, the near-field mode density is controlled in a nanoparticle dimer resonator in the same manner as the far-field mode density in a macroscopic cavity resonator.

Experimental work on fluorescence inside nanoparticle dimer resonators has recently begun. Up to now, strong enhancements of the fluorescence intensity and of the overall decay rate have been reported [8]. In this Letter, we report shaping of fluorescence emission spectra within single nanosized dimer resonators. The change in the shape of the emission spectra is purely due to the change in spontaneous emission rates and allows to directly test theoretical predictions of the emission rate enhancement factor [9]. Generalized Mie theory calculations quantitatively confirm that modifying the resonator length by a few nanometers leads to a drastic change of the fluorescence spectrum [Fig. 1(a)], if and only if the multilevel nature of the fluorophore is taken into account.

Nanoparticle dimer resonators with embedded fluorophores are prepared from gold nanoparticles coated with about 75 active antidigoxigenin antibodies as shown in Fig. 1(b). Bovine serum albumin (BSA) molecules functionalized with, on average, 2.5 digoxigenin molecules (Dig) and 2.5 Cy3 fluorescent dye molecules are added as linkers to an aqueous solution of the nanoparticles. As more than one antibody-coated gold nanoparticle can bind to a given BSA, either strong or weak aggregation of the nanoparticles results, depending on the relative concentrations of nanoparticles and BSA. The maximum dimer yield was obtained using a large excess of functionalized BSA (10000:1) at a nanoparticle concentration of $c = 6.1 \times 10^{-10}$ mol/L. The dimer solution is purified by gel electrophoresis as described elsewhere [7]. Because of different linker geometries, the dimers show varying surface-to-surface distances. On 28 dimers investigated

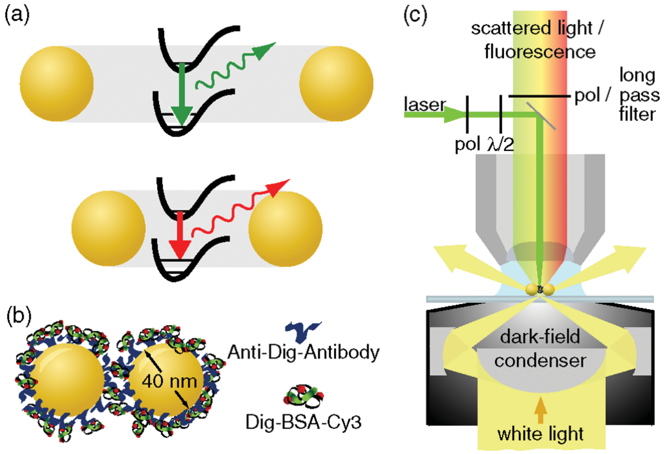

FIG. 1 (color). (a) Radiative transitions to different ground state sublevels are enhanced in dimer resonators of different lengths. (b) Plasmonic nanoresonators with embedded fluorescent molecules. (c) Experimental setup.

by transmission electron microscopy [10], we observed interparticle distances between 1.2 and 13.3 nm, so that a wide range of resonance frequencies could be realized.

The dimers are investigated spectroscopically using the light microscope shown schematically in Fig. 1(c), which allows us to acquire consecutively scattering and fluorescence spectra of the same nano-object. First, the resonance frequency of the nanoresonators is determined by scattering spectroscopy. The dimers are immobilized on a glass cover slip and immersed in water. A dark field condenser ($\mathrm{NA} = 1.2$–1.4) focuses white light of a halogen lamp on a single dimer. Scattered light is collected by a water immersion objective lens ($\mathrm{NA} = 1.0$), polarization analyzed, spectrally resolved with a grating spectrometer, and recorded with a CCD camera. The nanoresonator orientation can be determined from the polarizer angle that maximizes the scattering intensity, since the longitudinal plasmon mode scatters more strongly.

Subsequently, fluorescence of the dye molecules embedded in the same nanoresonator is measured by exciting in epifluorescence geometry with laser light at $\lambda = 532$ nm, polarized along the dimer axis. The low excitation intensity of $I_{\mathrm{exc}} = 0.6\ \mu\mathrm{W}/(\mu\mathrm{m})^2$ prevents Raman-induced motion of the nanoparticles [7,10]. The polarization analyzer is replaced by a long pass edge filter that blocks elastically scattered laser light.

Figures 2(a) and 2(b) visualize our experimental results. They show how the plasmonic nanoresonators coerce embedded Cy3 molecules into emitting at the resonators' frequencies, and thus reshape the fluorescence emission spectra. The nanoresonators are characterized with scattering spectroscopy of the longitudinal plasmon [Fig. 2(a)]. As the distance between the two nanoparticles decreases, the coupling between their plasmons becomes stronger, leading to an increasing redshift of the longitudinal mode resonance. Four representative scattering spectra are shown in Fig. 2(a). Figure 2(b) shows the corresponding fluorescence spectra. Comparing Figs. 2(a) and 2(b), we clearly see how the dye molecules are forced to emit preferentially at the resonance frequency of the nanoparticle dimers. This drastically changes and in some cases even reverses the relative intensities of the vibrational subbands.

We model the experimental situation as part of the more general problem of fluorescence enhancement by an aggregate of an arbitrary number of spherical nanoparticles, which we treat in the framework of generalized Mie theory as formulated by Xu [11]. The nanoparticles are modeled as homogeneous, isotropic spheres whose electromagnetic properties are given by their dielectric function. The fluorescent molecule is modeled by means of a Hertzian dipole with dipole moment $\mathbf{p}$. A similar treatment has previously been given for surface-enhanced Raman scattering near a single nanoparticle and near nanoparticle dimers [12].

The goal of the calculation is to obtain the frequency-dependent fluorescence enhancement $g(\omega)$ near an aggregate of N spherical nanoparticles, where the choice of the term "enhancement" is not meant to exclude $g(\omega) < 1$. Excitation and emission are considered here as two independent processes occurring at different wavelengths.

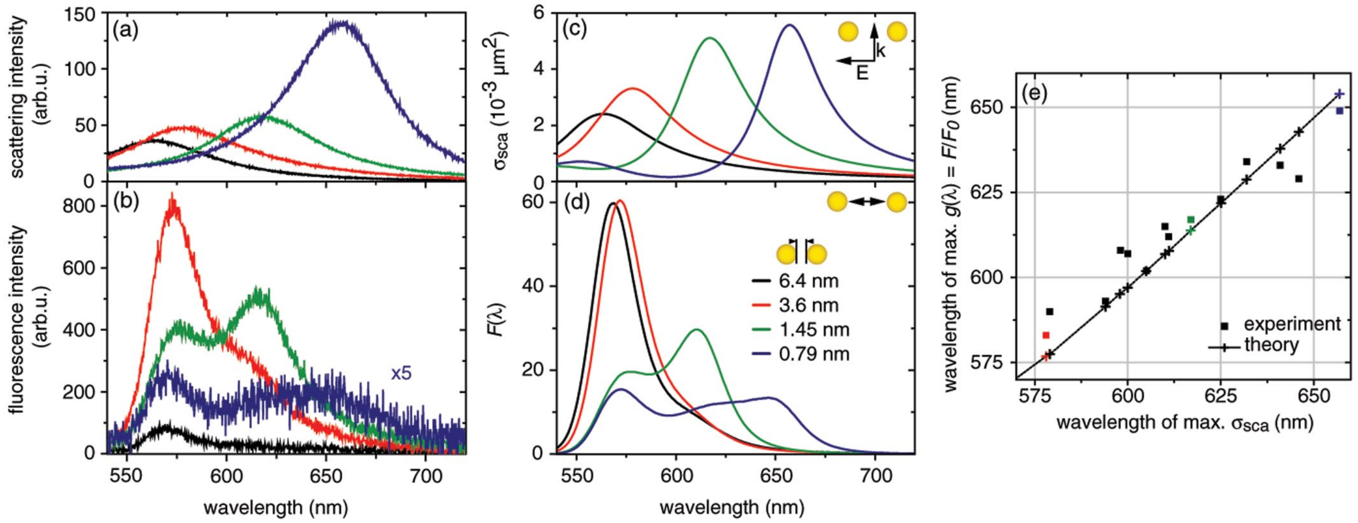

FIG. 2 (color). Experimental (a),(b) and theoretical (c),(d) scattering and fluorescence spectra of nanoparticle dimer resonators with incorporated Cy3 dye molecules. The nanoresonators shape the fluorescence spectra by favoring specific resonant transitions. (a) Experimental scattering spectra and (b) experimental fluorescence spectra of single dimers; spectra with identical colors are measured on the same dimer. (c) Theoretical plane wave scattering cross sections of nanoparticle dimers whose interparticle distance is chosen such that the resonance wavelengths are those of (a). (d) Enhanced fluorescence spectra for Cy3 molecules located in the center of the same dimers calculated according to Eq. (5); the molecular dipole is oriented along the dimer axis [10]. (e) Experimental (■) and theoretical (+) correlation between the wavelengths of maximum fluorescence enhancement and the wavelengths of maximum scattering, which indicate the resonance wavelengths of the nanoresonators.

Accordingly, we split the total enhancement into an excitation enhancement $g_{\mathrm{exc}}(\omega_{\mathrm{exc}})$ and an emission enhancement $g_{\mathrm{em}}(\omega)$ as

$$g(\omega) = g_{\mathrm{exc}}(\omega_{\mathrm{exc}}) g_{\mathrm{em}}(\omega). \tag{1}$$

We first calculate the excitation enhancement factor g_{exc} by exposing the nanoparticle aggregate to an incident plane wave $\mathbf{E_0}(\mathbf{r}, t) = \mathbf{E_0} \exp[-i(\omega_{\mathrm{exc}} t - kz)]$, where k is the wave number in the medium. Generalized Mie theory gives the partial scattered fields $\mathbf{E}^j_{\mathrm{sca}}$ for all spheres [11]. The local field at the location of the dipole $\mathbf{r}_0$ is then obtained as the sum $\mathbf{E}(\mathbf{r}_0) = \mathbf{E_0}(\mathbf{r}_0) + \sum_{j=1}^N \mathbf{E}^j_{\mathrm{sca}}(\mathbf{r}_0)$ and the excitation enhancement is given by

$$g_{\mathrm{exc}}(\omega_{\mathrm{exc}}) = \frac{|\mathbf{p} \cdot \mathbf{E}(\mathbf{r}_0)|^2}{|\mathbf{p} \cdot \mathbf{E}_0(\mathbf{r}_0)|^2}. \tag{2}$$

We now calculate the frequency-dependent emission enhancement factor $g_{\mathrm{em}}(\omega)$. We first let the field of a dipole situated at $\mathbf{r}_0$ and emitting at frequency ω interact with the nanoparticle aggregate. Using generalized Mie theory, we calculate the far-field radiated power P_r and the power absorbed by the nanoparticles P_{abs}. The decay rates of a dipolar two-level system with transition frequency ω due to photon emission Γ_r and due to energy transfer to the coupled plasmon of the nanoparticles Γ_{ET} are then given by $\Gamma_r = P_r/(\hbar\omega)$ and $\Gamma_{\mathrm{ET}} = P_{\mathrm{abs}}/(\hbar\omega)$. We normalize these rates to the radiative rate Γ_0 of the isolated dipole, which we derive from its radiated power P_0 as $\Gamma_0 = P_0/(\hbar\omega)$, and we obtain the enhancement factor of the radiative rate $g_r(\omega) = \Gamma_r/\Gamma_0$ and the energy transfer factor $g_{\mathrm{ET}}(\omega) = \Gamma_{\mathrm{ET}}/\Gamma_0$. The spectral probability density $\Pi(\omega)$ for an excited dye molecule in the aggregate to relax by the emission of a photon of a specific frequency ω is then given by

$$\Pi(\omega) = \frac{\gamma_{r0} f_0(\omega) g_r(\omega)}{\gamma_r + \gamma_{\mathrm{ET}} + \gamma_{\mathrm{nr0}}}, \tag{3}$$

where γ_{r0} and γ_{nr0} are the radiative and nonradiative decay rates of the isolated molecule, respectively, and $f_0(\omega)$ is the integral-normalized fluorescence spectrum of the isolated molecule. The total emission and energy transfer rates, γ_r and γ_{ET}, are given by the integrals $\gamma_r = \gamma_{r0} \int_0^\infty f_0(\omega) g_r(\omega) d\omega$ and $\gamma_{\mathrm{ET}} = \gamma_{r0} \int_0^\infty f_0(\omega) g_{\mathrm{ET}}(\omega) d\omega$, since the electronic inhomogeneity in a liquid environment is randomized on a time scale smaller than the excited state lifetime [13]. The emission enhancement factor at frequency ω is then given by

$$g_{\mathrm{em}}(\omega) = \frac{\Pi(\omega)}{\eta_0 f_0(\omega)}, \tag{4}$$

where η_0 is the quantum efficiency of the isolated molecule. From Eqs. (1), (3), and (4) we now see that the spectral dependence of the total fluorescence enhancement $g(\omega)$ is determined solely by the enhancement factor of the radiative decay rate $g_r(\omega)$.

Finally, the fluorescence emission spectrum of the molecule in the aggregate is obtained as

$$F(\omega) = g(\omega) F_0(\omega), \tag{5}$$

where $F_0(\omega) = f_0(\omega)/f_0(\omega_{\max})$ is the amplitude-normalized emission spectrum of the molecule in absence of the aggregate.

We have thus reduced the problem to the calculation of the radiated and absorbed powers P_r and P_{abs}. To this end, the incident dipole field [14] is first expanded in vector spherical harmonics $\mathbf{N}^{30}_{mn}$, $\mathbf{M}^{30}_{mn}$ in the coordinate system centered at the dipole, which yields the expansion coefficients a^0_{mn}, b^0_{mn}. From these, vector translation theorems [15] give the coefficients p^j_{mn}, q^j_{mn} of the expansion of the dipole field in vector spherical harmonics $\mathbf{N}^{1j}_{mn}$, $\mathbf{M}^{1j}_{mn}$ in the coordinate systems of spheres j, for $1 \le j \le N$. The scattering equations are solved neglecting feedback from the spheres to the dipole, which is small [12,16], and we obtain the partial scattering coefficients in addition to the incident wave expansion coefficients. From these the scattering and extinction cross sections σ_{sca}, σ_{ext} can be calculated analytically as shown by Xu [11]. The powers P_{sca}, P_{ext} are related to the corresponding cross sections by

$$\frac{P_{\mathrm{sca,ext}}}{P_0} = \frac{3}{2} \frac{\sigma_{\mathrm{sca,ext}}}{4\pi} k^2. \tag{6}$$

The far-field radiated power P_r is calculated using Xu's formula for the scattering cross section [11] with the modification that the sums over the sphere index start at index 0 to include the coefficients a^0_{mn}, b^0_{mn} of the primary dipole field. The absorbed power $P_{\mathrm{abs}} = P_{\mathrm{ext}} - P_{\mathrm{sca}}$ is calculated with Xu's expressions for the extinction and scattering cross sections [11].

Figure 2(c) shows longitudinal-mode scattering cross sections calculated using generalized Mie theory for two nanoparticles of 40 nm diameter immersed in water. The distances between the nanoparticles are chosen such that the experimental scattering peak positions of Fig. 2(a) are reproduced. The interparticle distances of 6.4, 3.6, 1.45, and 0.794 nm thus deduced will slightly underestimate the real interparticle distance because we neglect the larger refractive index of the protein layer and substrate (both have $n \approx 1.5$). However, the correlation between resonance frequency and maximum fluorescence enhancement is not affected by this approximation.

Theoretical spectra $F(\omega)$ [Eq. (5)] of enhanced fluorescence for a molecule at the center of the nanoresonators of Fig. 2(c) are shown in Fig. 2(d). The intermediate steps of the calculation leading to Fig. 2(d), in particular $g_{\mathrm{exc}}(\omega_{\mathrm{exc}})$, $g_r(\omega)$, $g_{\mathrm{ET}}(\omega)$, $g_{\mathrm{em}}(\omega)$, and $g(\omega)$, can be found in the supporting material [10]. The parameters entering the calculation are (i) the measured intrinsic fluorescence spectrum of Cy3, the measured intrinsic quantum yield of Cy3, and the nanoparticle diameter of 40 nm determined by TEM [10]; (ii) literature dielectric functions of water and gold [17]; (iii) the excitation wavelength of 532 nm selected in the experiment with a narrow bandpass filter; and (iv) the interparticle distances deduced by comparing measured and calculated scattering spectra. Thus, there are no free parameters in the calculation of $F(\omega)$.

The shapes of the theoretical spectra are in good agreement with those of the experimentally measured enhanced fluorescence spectra in Fig. 2(b). This might seem surprising at first since the dye molecules in the experiment are distributed all over the sphere surface. But the molecules in the interparticle hot spot experience the strongest excitation enhancement and therefore dominate the ensemble emission spectrum. The overall intensity strongly depends on the number of molecules in each hot spot and is therefore subject to random variations. Because of dominant homogeneous broadening [13], the shape of the spectra does not depend on the number of emitting molecules, which explains the excellent agreement between experiment and theory with respect to the spectral shape.

The correlation between the wavelengths of maximum fluorescence enhancement $g(\omega)$ and the resonance wavelengths of the plasmonic nanoresonators extracted from their scattering spectra is shown in Fig. 2(e). Theoretical and experimental correlations are in excellent agreement. Both are almost linear with a slope of $m \approx 0.95$. This shows that the nanoresonator selectively enhances the probability of resonant transitions. At any one point in time, an excited molecule is more likely to relax into a particular vibrational sublevel of the electronic ground state if the transition to that level is in resonance with the plasmonic resonator. While the molecule is in the excited state its electronic configuration fluctuates due to the fluctuating liquid environment. Seen over time, the molecule is more likely to emit when one of its fluctuating transition frequencies hits the plasmonic resonance.

In conclusion, we have shown both theoretically and experimentally how plasmonic nanoresonators, with dimensions much smaller than the wavelength, shape the emission spectra of fluorescent molecules through the selective, resonant enhancement of radiative transitions. Similar to the distance between the mirrors of macroscopic resonators, the distance of two nanoparticles serves to tune the nanoparticle dimer resonator. The spectral variation of the fluorescence enhancement factor is solely determined by the enhancement factor of the radiative decay rate. Thus our experiment also constitutes the first direct measurement of radiative decay rate enhancement in a single plasmonic nanoresonator.

This work has been supported by the Bavarian Science Foundation and by the Deutsche Forschungsgemeinschaft through SFB 486, the Gottfried-Wilhelm-Leibniz Program, and the Nanosystems Initiative Munich (NIM).

---

*feldmann@lmu.de

[1] E. M. Purcell, Phys. Rev. **69**, 681 (1946).

[2] K. H. Drexhage, H. Kuhn, and F. P. Schäfer, Ber. Bunsen-Ges. Phys. Chem. **72**, 329 (1968); D. J. Heinzen *et al.*, Phys. Rev. Lett. **58**, 1320 (1987); F. De Martini *et al.*, Phys. Rev. Lett. **59**, 2955 (1987).

[3] H. Yokoyama *et al.*, Appl. Phys. Lett. **57**, 2814 (1990); M. Suzuki *et al.*, Appl. Phys. Lett. **58**, 998 (1991).

[4] E. Dulkeith *et al.*, Phys. Rev. Lett. **89**, 203002 (2002).

[5] E. Le Ru *et al.*, J. Phys. Chem. C **111**, 16076 (2007).

[6] C. Sönnichsen *et al.*, Nat. Biotechnol. **23**, 741 (2005).

[7] M. Ringler *et al.*, Nano Lett. **7**, 2753 (2007).

[8] J. N. Farahani *et al.*, Phys. Rev. Lett. **95**, 017402 (2005); J. Zhang *et al.*, Nano Lett. **7**, 2101 (2007); O. Muskens *et al.*, Nano Lett. **7**, 2871 (2007); A. Bek *et al.*, Nano Lett. **8**, 485 (2008).

[9] L. A. Blanco and F. J. Garcia de Abajo, Phys. Rev. B **69**, 205414 (2004); P. Johansson, H. Xu, and M. Kall, Phys. Rev. B **72**, 035427 (2005); L. Rogobete *et al.*, Opt. Lett. **32**, 1623 (2007); J.-W. Liaw, Jpn. J. Appl. Phys. **46**, 5373 (2007).

[10] See EPAPS Document No. E-PRLTAO-100-024821 for the TEM micrograph of a dimer, details of the calculation leading to Figs. 2(d) and 2(e) of this Letter, and a comparison of scattering spectra before and after the fluorescence measurement showing constant interparticle distance during the experiment. For more information on EPAPS, see http://www.aip.org/pubservs/epaps.html.

[11] Y.-L. Xu, Appl. Opt. **34**, 4573 (1995); **37**, 6494(E) (1998); **36**, 9496 (1997); Phys. Lett. A **249**, 30 (1998).

[12] M. Kerker, D.-S. Wang, and H. Chew, Appl. Opt. **19**, 4159 (1980); H. Xu *et al.*, Phys. Rev. E **62**, 4318 (2000); H. Xu, Ph.D. thesis, Chalmers University of Technology and Göteborg University, 2002.

[13] A. B. Myers, Annu. Rev. Phys. Chem. **49**, 267 (1998).

[14] J. A. Stratton, *Electromagnetic Theory* (McGraw-Hill, New York, 1941).

[15] S. Stein, Q. Appl. Math. **19**, 15 (1961); O. R. Cruzan, Q. Appl. Math. **20**, 33 (1962).

[16] P. Bharadwaj and L. Novotny, Opt. Express **15**, 14 266 (2007).

[17] P. B. Johnson and R. W. Christy, Phys. Rev. B **6**, 4370 (1972).